Comparison of Crystallization Behaviors of Poly(ε-caprolactone) in Confined Environment with that in Bulk

Tongfei Wu,[1,2] Xikui Zhang,[3] Guisheng Yang[1,3]

[1]Beijing National Laboratory for Molecular Science, CAS Key Laboratory of Engineering Plastics,
Joint Laboratory of Polymer Science and Technology, Institute of Chemistry, The Chinese Academy of Sciences,
Beijing 100080, China
[2]Graduate University of the Chinese Academy of Sciences, Beijing, 100039, China
[3]Shanghai Genius Advanced Materials Co., Ltd., Shanghai 201109, China

ABSTRACT: The spatial confinement of poly(ε-caprolactone) (PCL) in the matrix of PMMA was synthesized by *in situ* polymerization and characterized by WAXD and SEM. The nonisothermal crystallization behavior and the kinetics of PCL in PMMA/PCL (85/15) blend and pure PCL were investigated by means of DSC. Jeziorny and Ozawa's theoretical prediction methods were used to analyze the crystallization kinetics. The melting behavior after cooling was also studied. There was an additional interesting phenomenon of double-melting peak for pure PCL. Peaks at lower temperature shifted to lower temperature, and peaks at higher temperature did not shift with the increasing cooling rate. This behavior can be due to recrystallization. For the high-crystallization activity energy and low-crystallization rate, PCL in bulk would recrystallize during the melting process, and displayed a double-melting behavior. Under spatial confinement of the rigid PMMA, PCL had much lower crystallization activity energy and had only one melting peak. © 2007 Wiley Periodicals, Inc. J Appl Polym Sci 107: 3796–3803, 2008

Key words: PMMA/PCL blend; spatial confinement; nonisothermal crystallization kinetics; recrystallization

INTRODUCTION

Even though semicrystalline polymers are widely used nowadays, some aspects of polymer crystallization are yet poorly understood.[1–5] Poly(ε-caprolactone) (PCL) is a well-known, biodegradable, and semicrystalline aliphatic polyester with interesting properties and applications in the biomedical field.[6,7] According to a theory that a biodegradable phase is dispersed in a continuous biostable acrylic matrix, and its biodegradation allows the ingrowth of osseous tissue inside the implanted devices during the repairing healing process,[8] its blends with PMMA were expected to be a good candidate for self-curing acrylic-based bone cements, and were well investigated as a medical material. However, few studies about crystallization of PCL in the matrix of PMMA were reported. And the crystallization behavior of PCL affects much on its biodegradation rate. Massa and Dalkoni-Veress' study[9] suggested that the crystallizable volume plays a crucial role in the crystallization process. Isolated in a confinement volume, the crystallization behavior of a polymer changes when compared with that of its bulk.[10]

In this work, spatial confinement of PCL in the matrix of PMMA was generated by *in situ* polymerization and characterized by SEM, WAXD, and DSC. We focus on confined systems since they can provide a deep understanding of crystallization processes inside this material, because the confinement volume approaches intrinsic lengths of the phenomenon studied.[5,11] In this article, the crystallization activity energy of PCL under spatial confinement was shown much lower than that of PCL in bulk, and this provides a model to explain the phenomenon of double-melting peak for PCL. The nonisothermal crystallization kinetics of PCL in bulk and PMMA/PCL (85/15) blend was investigated by two kinetic approaches which have been proposed to predict and analyze nonisothermal crystallization kinetics.

EXPERIMENTAL

Material and preparation

Methyl methacrylate (MMA) purchased from Sinopharm Chemical Reagent (Shanghai, China) was purified by vacuum distillation. 2,2'-Azo-bis-iso-

butyronitrile (ABIN) was used as initiator for acrylic polymerization. PCL (M_w = 50,000 g/mol) was received from Tianshengcheng (Wuhan, China).

PMMA-based blend was synthesized starting from the mixture of MMA monomer and PCL in a proportion (MMA/PCL weight ratio: 85/15). In a boiling flask equipped with a condenser-Allihn type, the PCL was first dissolved in MMA at 100°C, which is the boiling point of MMA, under vigorous stirring and left for 2 h. Afterward, an amount of ABIN (0.2 wt % relative to MMA) was added and the polymerization was carried out with tenderly mechanical stirring approximately for 30 min at 80°C, followed by a curing cycle in a thermostatic oven at 45°C for 16 h. After an anneal program at 100°C for 2 h, the blends were obtained.

Morphology

Samples, fractured in liquid N_2, were dipped in 0.1N H_2SO_4 for 30 days, then surface-coated with a thin layer of Au and observed using a scanning electron microscope LV-5600 (JEOL, Japan), operating at 10 kV.

Differential scanning calorimetry measurements

The calorimetric measurements of pure PCL and PMMA/PCL (85/15) blend were conducted on a TA Q100 differential scanning calorimeter in a dry nitrogen atmosphere. The apparatus was calibrated using indium and zinc standards for calibration for low- and high-temperature regions, respectively. The weight of samples was about 5.0 mg for all the measurements. In the nonisothermal crystallization kinetics experiment, the samples were first heated to 100°C (below the transition temperature T_g of PMMA, which is identified to be 109°C) at a heating rate of 10°C/min and held at this temperature for 3 min to eliminate all effects of past thermal history. Then, they were cooled to −40°C at cooling rates of 5, 10, 20, and 40°C/min, and the heat flow during crystallization was recorded as a function of time.

The relative crystallinity, X_t of PCL can be calculated using the following equation:

$$X_t = \frac{\int_{t_0}^{t} \frac{dH}{dt} dt}{\int_{t_0}^{\infty} \frac{dH}{dt} dt} \times 100\% \qquad (1)$$

where t_0 and t are the temperatures at which crystallization starts and ends, respectively.

Wide-angle X-ray diffraction

Rigaku D/Max-III X-ray diffractometer was used to determine crystalline structure of pure PCL and PMMA/PCL (85/15) blend. The X-ray wavelength was 0.154 nm, the scanning speed was 8°/min, and the scanning range of 2θ was from 0° to 50°. All the measurements were performed at room temperature.

The distance between crystalline planes (hkl), d is given by the well-known Bragg's equation:

$$2d \sin \theta = \lambda \qquad (2)$$

where λ is the X-ray wavelength, equal to 0.154 nm; θ is Bragg angle.

The crystallite size perpendicular to the plane (hkl), D_{hkl} is usually given by the Scherrer equation:

$$D_{hkl} = K\lambda/(\beta \cos \theta) \qquad (3)$$

where K is the Scherrer shape factor, here K = 0.9; λ is the X-ray wavelength; θ is Bragg angle; β is the pure line broadening, which is calculated from the assumptive relation: $\beta^2 = (B^2 - b_0^2)$, where B is the measured half-width of the experiment profile (in degrees); b_0 is the instrumental broadening, which was found to be 0.15° from scans of standard silicon power.

RESULTS AND DISCUSSION

Spatial confinement

Figure 1 shows a spherical profile of PCL with almost monodistributed dimensions, about 2 μm, after selectively removing the PCL component distributed in the matrix of PMMA. The monodistributing indicates that the blend must suffer a viscoelastic phase separation. The values of the crystallite size (D_{hkl}) perpendicular to the plane (hkl) in pure PCL and PMMA/PCL (85/15) blend are presented in Table I. It shows that the crystallite sizes of PCL perpendicular to the planes (110) and (200) are both smaller in PMMA/PCL blend than that in pure PCL, that is, the crystallite size of PCL distributed in the matrix of PMMA became smaller than that in bulk. The reason for this phenomenon is that the poorly crystallized macromolecules or small and metastable crystals were strictly confined by the rigid PMMA matrix. The values of distance between crystal planes (d_{hkl}) in Table I and WAXD patterns for pure PCL and PMMA/PCL blend in Figure 2 indicate that the crystal structure of PCL in PMMA/PCL blend has not changed.

Nonisothermal crystallization behavior

Figure 3 shows the cooling thermograms during nonisothermal crystallization process at various cooling rates for the pure PCL and PMMA/PCL (85/15) blend. The exothermic peaks become wider and shift
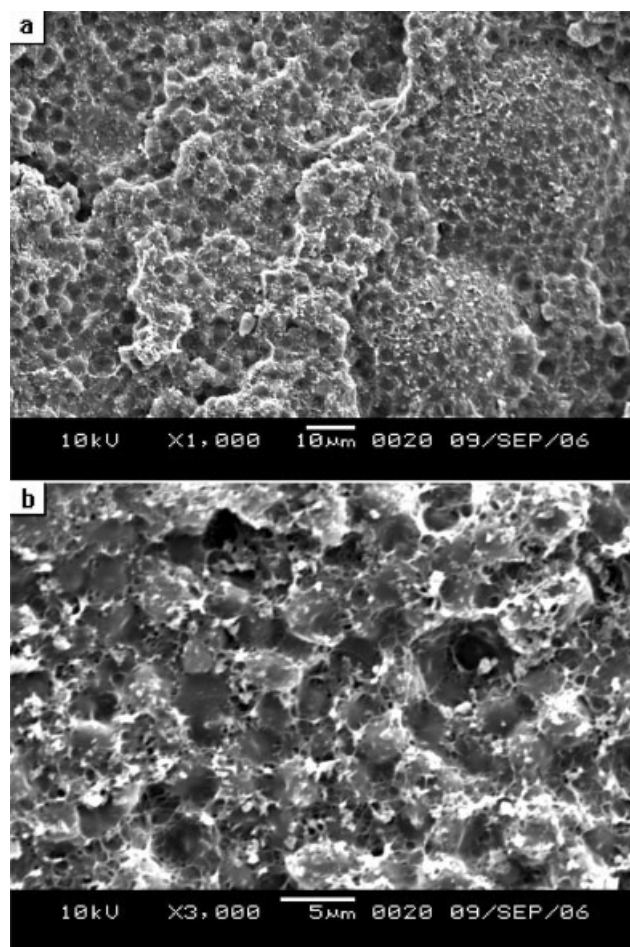
Figure 1 SEM microphotographs of free-fractured surfaces of PMMA/PCL (85/15) blend at two different magnifications.

to lower temperature as the cooling rate increased. But the exothermic peak has a further shift in PMMA/PCL (85/15) blend than that in pure PCL.

From the nonisothermal DSC thermograms at various cooling rates, several values of crystallization parameters can be obtained. The onset crystallization temperature (T_o), maximum crystallization rate temperature (T_p), time (t_{max}), undercooling temperature (ΔT_c), and crystallization enthalpy (ΔH_c), are sum-

TABLE I
The Distance Between Crystal Planes (d_{hkl}) and Crystallite Size (D_{hkl}) of PCL in Pure PCL and PMMA/PCL (85/15) Blend

	PCL (wt %)	$2\theta^a$	B^b	β^c	d_{hkl} (nm)	D_{hkl} (nm)
L110	100	21.34	0.38	0.35	0.42	0.40
	15	21.18	0.43	0.40	0.42	0.35
L200	100	23.62	0.40	0.37	0.38	0.38
	15	23.42	0.48	0.45	0.38	0.31

[a] Bragg angle.
[b] Measured half-width of the experimental profile.
[c] Pure line broadening.

marized in Table II. With the cooling rate increasing, T_o, T_p, and t_{max} decrease, suggesting that a higher cooling rate requires a shorter crystalline period.

In addition, the crystallization rate, t_{max}^{-1} increases with the increase of the cooling rate, showing nucleation control of crystallization in both samples.

T_o and T_p of pure PCL was higher than that of PMMA/PCL (85/15) at given cooling rate, and the values of the differences for T_o and T_p between two samples at given cooling rate increased with the cooling rate increasing. There was a more sensitive influence of cooling rate on that of PMMA/PCL (85/15) than pure PCL, indicating the effect of dominance of both nucleation and growth processes in PMMA/PCL (85/15). The polymer chains in PMMA/PCL (85/15) had more mobility, and the growth rate became greater and comparable to nucleation, as concluded from ΔE discussed *infra*.

The evolution of the relative crystallinity, X_t was plotted as a function of crystallization temperature (T) for pure PCL and PMMA/PCL (85/15) blend, which are shown in Figure 4. The characteristic sigmoid curves suggest the lag effect of cooling rates upon crystallization.[12]

Furthermore, the X_t versus T curves can be converted into the dependence of the relative crystallinity as a function of time in terms of the following time–temperature transformation equation:

$$t = (T_o - T)/\Phi \qquad (4)$$

where T_o is the temperature when crystallization begins, T is the temperature at crystallization time t, and Φ is the cooling rate. The plots of the X_t versus time t are shown in Figure 5. Sigmoidel curves were
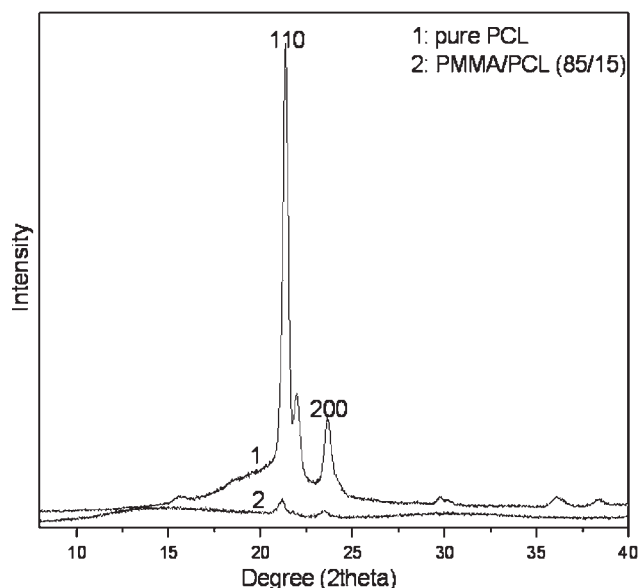
Figure 2 WAXD patterns for pure PCL and PMMA/PCL blend.
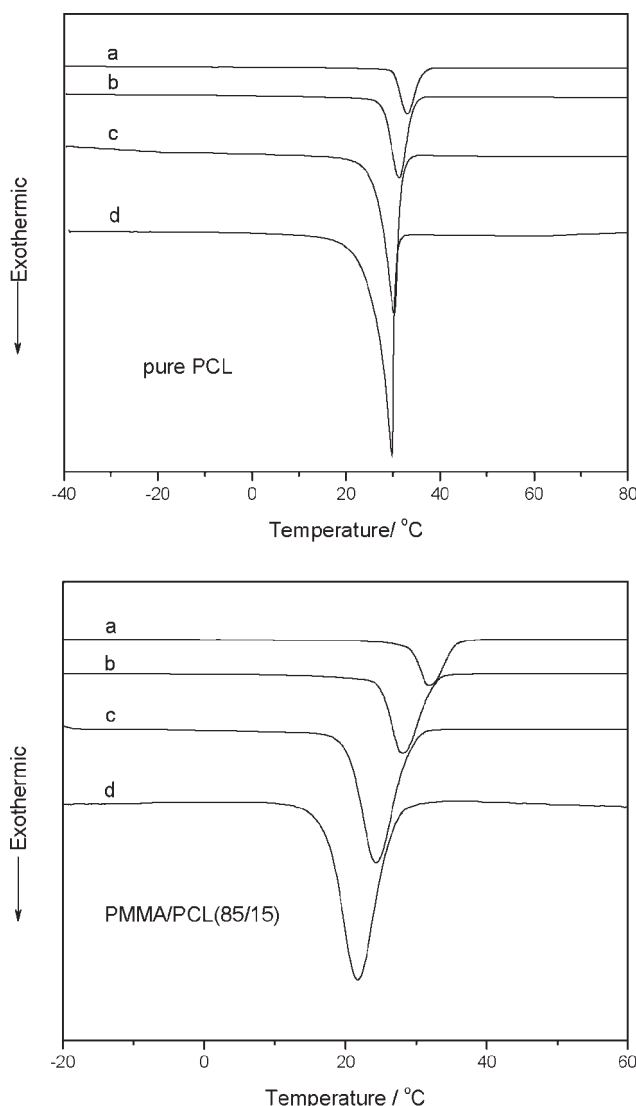
Figure 3 Cooling thermograms during nonisothermal crystallization at various cooling rates by DSC for the pure PCL and PMMA/PCL (85/15) blend: (a) 5°C/min, (b) 10°C/min, (c) 20°C/min, and (d) 40°C/min.

observed for pure PCL and PMMA/PCL (85/15) blend. It is seen that lower the cooling rate, the larger is the time range over which the crystalliza-

tion occurs, indicating that the crystallization is controlled by nucleation, as concluded from t_{max}^{-1} above.

Nonisothermal crystallization kinetics

The nonisothermal crystallization kinetics analysis is of practical importance since it can reflect the crystallization behavior of polymers under processing conditions. Several theoretical methods have been proposed to predict and analyze nonisothermal crystallization kinetics. Herewith, we adopted the Jeziorny and Ozawa theoretical methods to analyze the characteristics of nonisothermal crystallization kinetics for pure PCL and PMMA/PCL (85/15) blend. Finally, the activation energy ΔE was calculated using Kissinger's method.

Avrami equation by Jeziorny modified

Jeziorny considered that the primary stage of nonisothermal crystallization could be described by the Avrami equation at a constant cooling rate.[13] He obtained the following equation:

$$1 - X_t = \exp(-Z_t t^n) \tag{5}$$

where Z_t is the primary composite rate constant in the nonisothermal crystallization process, and it should be corrected by the cooling rate Φ. The final form of the rate parameter characterizing the kinetics of nonisothermal crystallization is given as follows:

$$\ln Z_c = \ln Z_t / \Phi \tag{6}$$

Drawing the straight line corresponding to $\ln[-\ln(1 - X_t)]$ versus $\ln t$ by using eq. (5), we can determine the value of the Avrami exponent n and the rate parameter Z_t from the slope and the intercept, respectively, (Fig. 6). The values of n and Z_c are shown in Table III.

The average value of the Avrami exponent was n_1 = 4.2 and 4.0 for pure PCL and PMMA/PCL (85/

TABLE II
Nonisothermal Crystallization Kinetic Parameters at Various Cooling Rates for the Pure PCL and PMMA/PCL (85/15) Blend

PMMA/PCL (w/w)	Φ (°C/min)	T_o (°C)	T_p (°C)	ΔH_c (J/g)	t_{max} (min)	ΔT_c (°C)
100/0	5	38.97	33.07	56.96	1.18	5.90
	10	36.9	31.36	56.46	0.55	5.54
	20	34.86	30.27	57.44	0.23	4.59
	40	32.62	29.83	56.92	0.07	2.79
85/15	5	35.48	31.77	5.16	0.74	3.71
	10	32.26	28.07	4.80	0.42	4.19
	20	28.86	24.4	4.95	0.22	4.46
	40	26.48	21.56	4.94	0.12	4.96
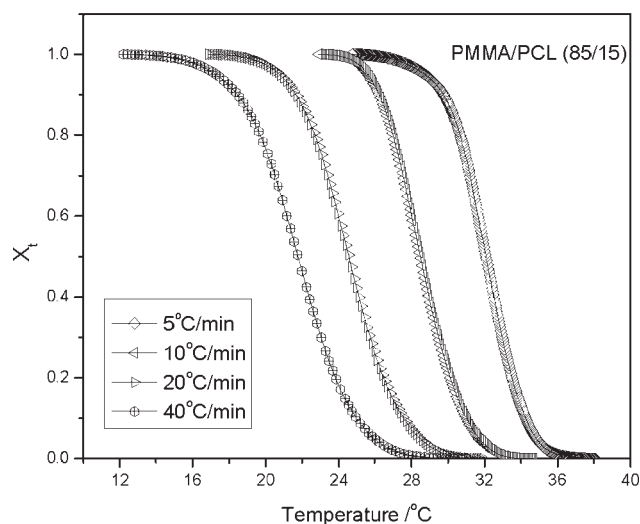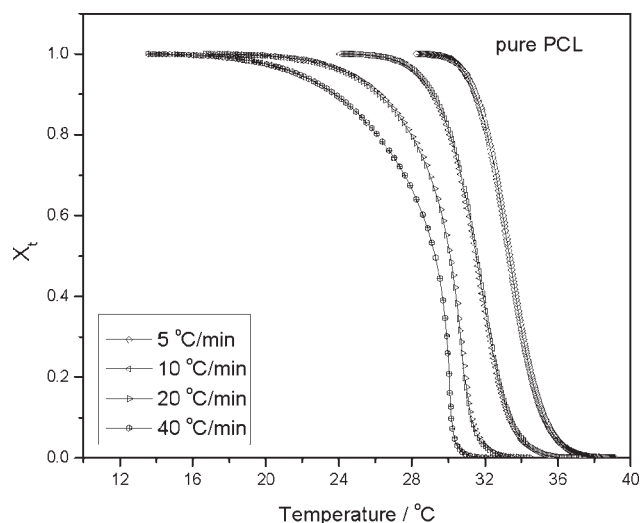
Figure 4 Plots of relative crystallinity (X_t) versus temperature (T) for the pure PCL and PMMA/PCL (85/15) blend crystallized nonisothermally at various cooling rates.

15) blend, respectively, which suggested that the primary crystallization stage for nonisothermal crystallization might correspond to a three-dimensional spherical growth with thermal nucleation.[14] In common, at the secondary stage, the form of spherulites' growth transformed into the lower dimensional space extension and the crystallization mode became simpler, which was considered to be due to the effect of the slower crystallization or further perfection of crystal, which were caused by the spherulite impingement or obstruction of rigid PMMA chains in the later stage of crystallization, or due to the reorganization of initially poorly crystallized macromolecules, or small and metastable crystals. Z_c is known as "the kinetic crystallizability." The larger the Z_c value, the higher is the crystallization rate. At the same cooling rate, the lower Z_{c1} of PCL in PMMA/PCL (85/15) than that of pure PCL indicates that the PMMA matrix impedes crystallization.
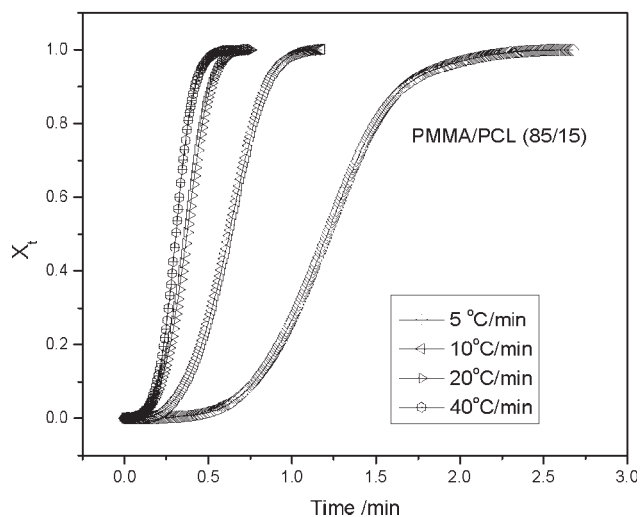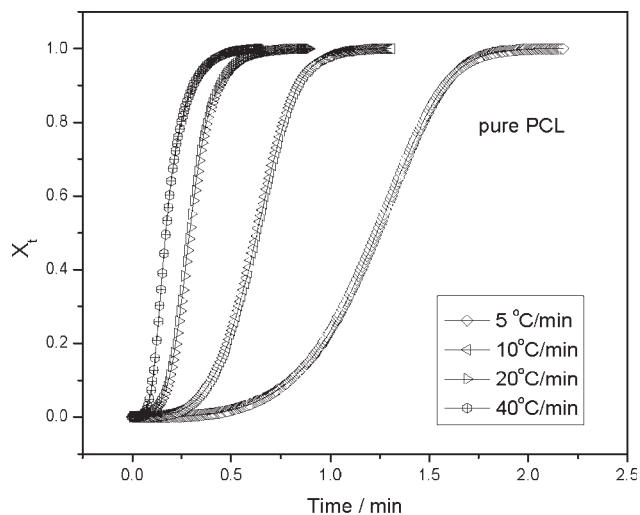
Ozawa equation in nonisothermal crystallization kinetics

Considering the effect of Φ, Ozawa modified eq. (4) to the Avrami eq. (5) and got the following for nonisothermal crystallization at T crystallization temperature[15]:

$$1 - X_t = \exp[-K(T)/\Phi^m] \qquad (7)$$

$$\ln[-\ln(1 - X_t)] = \ln K(T) - m \ln \Phi \qquad (8)$$

where m is the Ozawa exponent, and $K(T)$ is the kinetics crystallization rate constant. Drawing the plot of $\ln[-\ln(1 - X_t)]$ versus $\ln\Phi$ according to eq. (8), we should obtain a series of straight lines. The lines we obtained are shown in Figure 7. The values of m and $K(T)$ are shown in Table IV. From Figure 7,

Figure 5 Relation of relative crystallinity (X_t) as function of time (t) for the pure PCL and PMMA/PCL (85/15) blend at various cooling rates during nonisothermal crystallization.
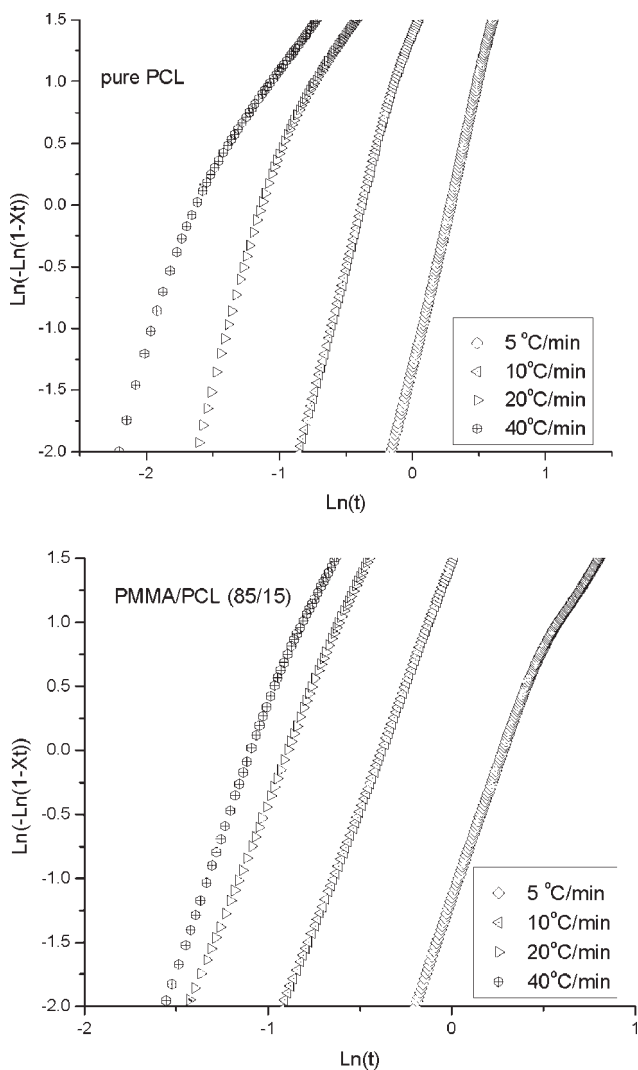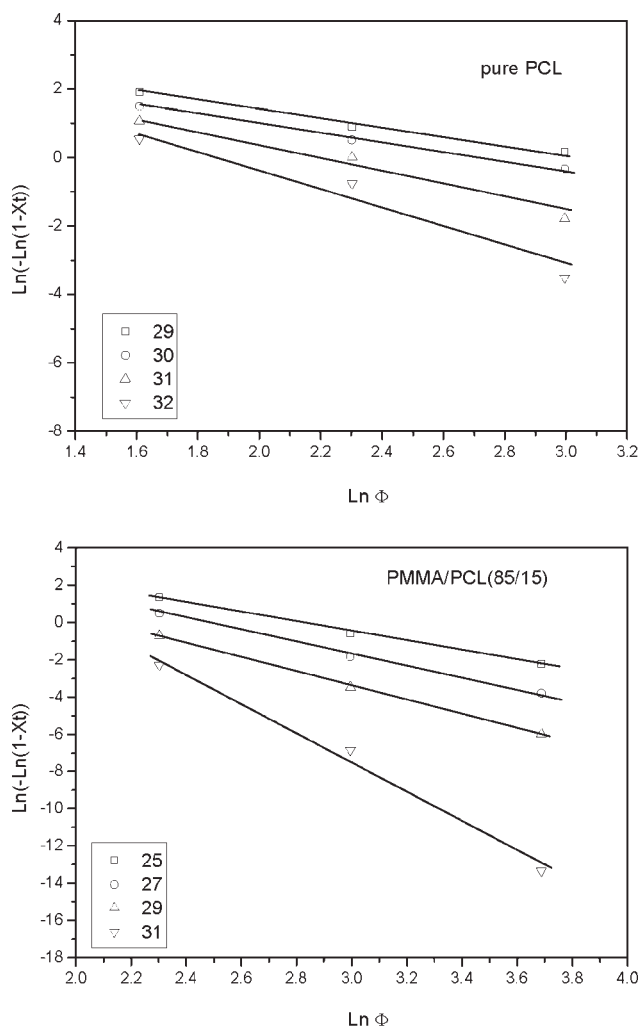
Figure 6 Plots of $\ln[-\ln(1 - X_t)]$ versus $\ln t$ during the nonisothermal crystallization process for pure PCL and PMMA/PCL (85/15) blend at indicated cooling rate.

Figure 7 The plot of $\ln[-\ln(1 - X_t)]$ versus $\ln\Phi$ from the Ozawa equation for pure PCL and PMMA/PCL (85/15) blend.

there is a good linear relation between $\ln[-\ln(1 - X_t)]$ and $\ln\Phi$, and it is evident that the Ozawa analysis could adequately describe the nonisothermal crystallization kinetics.

$K(T)$ is a function of temperature, related with the mode of nucleation, the nucleation rate, and the growth rate. Therefore, the value of $K(T)$ changes with the temperature increasing for both samples, indicating that the above factors of crystallization has changed. The exponent m increased as the crystallization temperature increased for both samples.

TABLE III
Parameters of Nonisothermal Crystallization Kinetics for PCL and PMMA/PCL (85/15) Blend

Sample	Φ (°C/min)	Primary stage N_1	Z_{c1}	Secondary stage N_2	Z_{c2}
Pure PCL	5	4.11	0.767	–	–
	10	4.24	1.171	2.62	1.147
	20	4.03	1.258	1.63	1.116
	40	4.49	1.155	1.50	1.066
PMMA/PCL (85/15) blend	5	4.17	0.792	2.21	0.943
	10	3.81	1.155	–	–
	20	3.62	1.174	–	–
	40	4.27	1.123	2.69	1.093

TABLE IV
The Ozawa Exponent m and the Ozawa Crystalline Rate Constant $K(T)$ for PCL and PMMA/PCL (85/15) Blend

Sample	T (°C)	m	$K(T)$
Pure PCL	29	1.25	49
	30	1.40	43
	31	2.05	89
	32	2.93	247
PMMA/PCL (85/15) blend	25	2.56	1,299
	27	3.10	1,939
	29	3.79	2,916
	31	7.96	5,833
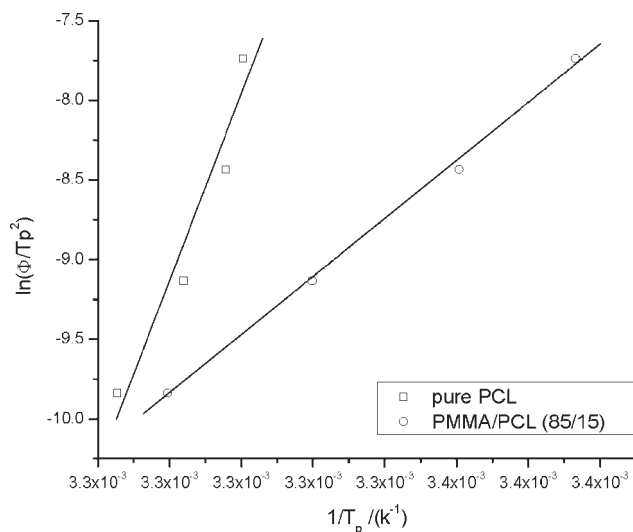
Figure 8 The plot of $\ln(\Phi/T_p^2)$ versus $1/T_p$ from the Kissinger method for pure PCL and PMMA/PCL (85/15) blend.

From Ozawa's theory, it could be derived that some so-called predetermined nuclei exist before cooling the melt; that is, there still existed a small quantity of unmolten residual crystal in the polymer.

Crystallization activation energy ΔE

Considering the influence of the various cooling rates Φ in the nonisothermal crystallization process, Kissinger thought the activation energy ΔE could be determined as follows[16]:

$$\frac{d(\ln\frac{\Phi}{T_p^2})}{d(\frac{1}{T_p})} = -\frac{\Delta E}{R} \qquad (9)$$

where R is the gas constant and T_p is the peak temperature.

Drawing a plot of $\ln(\Phi/T_p^2)$ versus $1/T_p$, we obtain a line with good linear relation in Figure 8; the slope = $d[\ln(\Phi/T_p^2)]/day(1/T_p)$ = $-\Delta E/2.303R$, ΔE = -1078.2, and -350.3 kJ/mol for pure PCL and PMMA/PCL (85/15) blend. Therefore, the crystallization activity energy for PCL droplets in the PMMA matrix is clearly lower than that for pure PCL, which could be explained as follows. ΔE is the activation energy required to transport molecular segments to the crystallization surface. The entanglement density played a main role in controlling the mobility of chains.[17] When PCL was segregated in the matrix of PMMA, the entanglement density would decrease, because a lot of entanglements existing in bulk would disappear, and the degree of decrease would be a function of dimensions of PCL. Furthermore, it is well known that the thermal history in the melt could affect the crystallization behavior of polymer. Thereby, unmolten crystalline

seeds or local chain organization could still remain at temperatures above the melting point. Accordingly, the presence of such primary nuclei decreases the crystallization free energy barrier and thus increases the crystallization rate. Such a phenomenon is also defined as self-nucleation.[18] The spatial confinement and graft may serve as an impetus to the local order section, which induced the melt crystallization. This would result in a decrease of crystallization free energy barrier; that is, their value of ΔE in magnitude for PCL in PMMA is much lower than that of pure PCL.

Melting behavior after cooling

The DSC thermograms of samples recorded at a heating rate of $10°C/min$ following nonisothermal crystallization are shown in Figure 9. T_m and ΔH_c of samples are shown in Table V. T_m of PMMA/PCL (85/15) are lower than that of pure PCL, which can be explained by a poor crystallization under the confinement. The
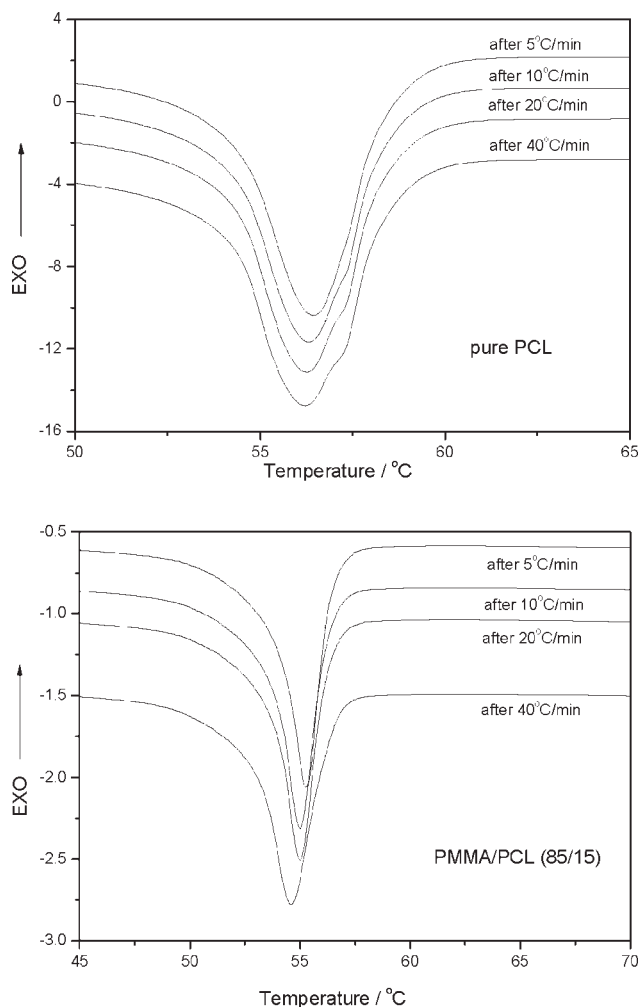
Figure 9 The DSC thermograms of samples recorded at a heating rate of $10°C/min$ following nonisothermal crystallization.

TABLE V
The Values of Melting Point (T_m) and Melting Enthalpy (ΔH_c) of Samples at a Heating Rate of 10°C/min After Nonisothermal Crystallization at Indicated Cooling Rate Φ

Sample	Φ (°C/min)	ΔH_c (J/g)	T_m (°C)	
Pure PCL	5	58.8	56.4	57.4
	10	61.1	56.3	57.4
	20	60.0	56.3	57.4
	40	60.5	56.2	57.4
PMMA/PCL (85/15) blend	5	4.9	55.3	
	10	4.6	55.0	
	20	4.9	55.0	
	40	5.0	54.6	

DSC thermograms of pure PCL exhibit two melting peaks, with the weak peak at a higher temperature, and this weak peak is swelling with the increasing cooling rate, while there is only one melting peak for PMMA/PCL (85/15). The well-defined double-melting peak has been discussed elsewhere, and this behavior of polymers in DSC experiments may be due to the following: (i) recrystallization effect, which arises from melting of imperfect crystals, followed by recrystallization into less imperfect crystals and then final melting; (ii) morphological effect, which implies melting of two populations of crystals, differing in both size and thickness, which will melt at two different temperatures. The later process takes place in amorphous regions containing both components, to which the noncrystallizable polymer migrates during the primary crystallization process.[19] However, there is a double-melting peak for pure PCL, which was also observed in another article.[20]

From Figure 9, the melting peak at lower temperature shifts to lower temperature with the increasing cooling rate. But there are no shifts of melting peak at higher temperature with the increasing cooling rate, indicating no influence of thermal histories, and these crystals should be formed in the melting process. When the cooling rate increases, more poor crystallization could be formed and more candidates could form less imperfect crystals as recrystallization. So the profile of this peak is swelling with the increasing cooling rate. PCL in PMMA/PCL (85/15) blend, with a lower crystallization free energy barrier, could form less imperfect crystals, resulting in only one melting peak.

CONCLUSIONS

PMMA/PCL (85/15) blend was synthesized by *in situ* polymerization and the spatial confinement of PCL in the matrix of PMMA was obtained and studied by SEM and WAXD. The nonisothermal crystallization behavior and the kinetics of the PCL in PMMA/PCL (85/15) blend were investigated by means of DSC. Jeziorny and Ozawa's theoretical prediction methods were used to analyze the crystallization kinetics. The results show that the Jeziorny method and Ozawa's theoretical method describing the nonisothermal crystallization kinetics of the PCL in both samples are practicable, but with different values of parameters. The melting behavior after cooling was also studied. There was an additional interesting phenomenon of double-melting peak for pure PCL. As peaks at lower temperature shifted to lower temperature and peaks at higher temperature did not shift with the increasing cooling rate, this behavior can be due to recrystallization. For the high-crystallization activity energy and low-crystallization rate, PCL in bulk would recrystallize during the melting process, and displayed a double-melting behavior. Under spatial confinement of the rigid PMMA, PCL had much lower crystallization activity energy and had only one melting peak.

References

1. Strobl, G. The Physics of Polymers. Concepts for Understanding Their Structures and Behavior; Springer: Berlin, 1997.
2. Strobl, G. Eur Phys J E 2000, 3, 165.
3. Lotz, B. Eur Phys J E 2000, 3, 185.
4. Muthukumar, M. Eur Phys J E 2000, 3, 199.
5. Reiter, G. J Polym Sci Part B: Polym Phys 2003, 41, 1869.
6. Pitt, C. G.; Chasalow, F. I.; Hibionada, Y. M.; Klimas, D. M.; Schindler, A. J Appl Polym Sci 1981, 26, 3779.
7. Perrin, D. E.; English, J. P. In Handbook of Biodegradable Polymers; Domb, A. J.; Kost, J.; Wiseman, D. M. Eds.; Harwood Academic Publishers: Singapore, 1977; Chapter 3.
8. San Roma'n, J.; Guille'n, P. In Biomaterial-Tissue Interfaces: Advances in Biomaterials; Doherty, P. J.; Williams, R. L.; Williams, D. F.; Lee, A. J. C., Eds.; Elsevier Science Publishers: Amsterdam, 1992; Vol. 10, p 459.
9. Massa, M. V.; Dalkoni-Veress, K. Phys Rev Lett 2004, 92, 255509.
10. Frensch, H.; Harnischfeger, P.; Jungnickel, B. J. In Multiphase Polymers: Blends and Ionomers; Utracki, L. A.; Weiss, R. A., Eds.; ACS Symposium Series; American Chemical Society: Washington, DC, 1989; p 395.
11. Massa, M. V.; Carvalho, J. L.; Dalnoki-Veressa, K. Eur Phys J E 2003, 12, 111.
12. Li, Z. M.; Yang, W.; Li, L. B.; Xie, B. H.; Huang, R.; Yang, M. B. J Polym Sci Part B: Polym Phys 2004, 42, 374.
13. Jeziorny, A. Polymer 1978, 19, 1142.
14. Wunderlich, B. Macromolecular Physics; Academic Press: New York, 1977; Vol. 2 Page 118.
15. Ozawa, T. Polymer 1971, 12, 150.
16. Kissinger, H. E. J Res Natl Bur Stand (US) 1956, 57, 217.
17. Ou-Yang, W.-C. Polym Int 1997, 29, 889.
18. Lee, Y.; Porter, R. S. Macromolecules 1988, 21, 2770.
19. Runt, J. P.; Harrison, I. R. In Methods of Experimental Physics; Fava, R., Ed.; Academic Press: New York, 1980; Vol. 16B, Chapter 9.
20. Vazquez-Torres, H.; Cruz-Ramos, C. A. J Appl Polym Sci 1994, 54, 1141.